ELSEVIER

Journal of Nuclear Materials 299 (2001) 124–131

journal of nuclear materials

www.elsevier.com/locate/jnucmat

Blister formation of tungsten due to ion bombardment

Wenmin Wang [a,b], J. Roth [a,*], S. Lindig [a], C.H. Wu [c]

[a] *Max-Planck-Institut für Plasmaphysik, EURATOM Association Boltzmannstrasse 2, D-85748 Garching, Germany*
[b] *Shanghai Institute of Nuclear Research, Academia Sinica, Shanghai 201800, People's Republic of China*
[c] *EFDA, Max-Planck-Institut für Plasmaphysik, D-85748 Garching, Germany*

Received 5 June 2001; accepted 14 August 2001

Abstract

Blisters formed at tungsten surfaces due to deuterium ion bombardment have been studied systematically in the energy range 100 eV to 1 keV. The bombardment with 1 keV D^+ at room temperature (RT) shows that the blister size increases and the number decreases with the deuterium fluence from 1×10^{19} to 1×10^{21} D^+/cm^2. No blisters are found at elevated temperatures between 600 and 800 °C. For bombardment with an energy as low as 100 eV, blisters are observed at the high fluence of 1×10^{21} D^+/cm^2. The blister size increases and the number decreases with the bombardment energy. Combined with scanning electron microscopy (SEM) ion beam depth profiling measurements have been used to investigate the effect of blister formation on the trapping behavior of deuterium in tungsten. Double implantations, where 4 keV He^+ and 100 eV D^+, respectively, were injected in W prior to the bombardment of 1 keV D^+ show a pronounced increase of deuterium retention and blister disappearance. Possible mechanisms are proposed to describe the observed phenomena.

1. Introduction

As early as 1970, the blister formation at the surface of various metals, such as Nb, Cu, Ni, stainless steel, due to light ion bombardment (H, D, He) was studied in detail theoretically and experimentally [1,2]. Recently, tungsten became one of the candidate plasma facing materials for fusion devices due to its low sputtering yield and good thermal properties. On the other hand, disadvantages have been pointed out, such as its high commercial price and ion-induced blister formation at the surface resulting in surface flaking. The reduced thermal contact of the flaked surface layers to the bulk may result in melting and evaporation due to high transient heat loads. The blister formation and hydrogen recycling through fissures in the blisters may affect the hydrogen transport and trapping properties, especially the tritium inventory in the future fusion machine. Some studies on hydrogen retention in W have been associated with the observation of blisters formed due to various conditions of hydrogen bombardment [3–5]. Haasz et al. [3] observed that the blisters formed at the tungsten surface due to 500 eV D^+ bombardment with a cumulative fluence of $>1 \times 10^{21}$ D^+/cm^2 result in a drastically reduced level of D retention for subsequent D fluences. Venhaus et al. [4] investigated the effects of pre-annealing temperature on the blister formation due to low energy bombardment of D and T. They also found that blister formation and rupture influence the retention of D and T.

Many studies on the trapping behavior of hydrogen isotopes in W have shown that the implanted H or D diffuses into the W bulk far beyond the ion projected ranges [3,6,7,17]. The investigation of the D trapping depth after blister formation could clarify the role of gas accumulation in cavities for blistering.

In the present work the formation of blisters at the W surface due to D bombardment has been systematically studied with different fluences, temperatures and energies by means of SEM and D depth profiling in order to have a good understanding of the blister formation mechanics and D trapping behavior.

* Corresponding author. Tel.: +49-89 3299 1387; fax: +49-89 3299 2279.
E-mail address: roth@ipp.mpg.de (J. Roth).

0022-3115/01/$ - see front matter
PII: S0022-3115(01)00679-1

2. Experimental

All the tungsten samples, 1 mm thick, 12×14 mm^2 with 99.99% purity, were mirror polished for the experiments. In order to study the surface damage in the materials as used in real plasma machines, two unpolished tungsten samples were bombarded with 300 eV and 3 keV D_3^+ up to the fluence of 1×10^{21} D^+/cm^2. The ion bombardment was carried out in a vacuum chamber connected to a high-current ion source [8]. The pressure was better than 1×10^{-7} Pa in the chamber, and increased to $(7–10) \times 10^{-5}$ Pa during bombardment. Prior to bombardment each sample was outgassed at 850 °C for 15 min. The ion exposure was performed at normal ion incidence for ion energies of 3 keV D_3^+ (1 keV/D^+), 600 eV D_3^+ (200 eV/D^+), and 300 eV D_3^+ (100 eV/D^+), with flux densities of 11, 5 and 6.25×10^{15} D^+/cm^2s, respectively. For a better ion source performance, 6, 3.6 and 3.3 keV ion beams were extracted from the ion source and decelerated in front of the samples by a positive target bias of 3 kV to achieve the 3 keV, 600 eV and 300 eV D_3^+, respectively. Different bombardment fluences of 1×10^{19} D^+/cm^2, 1×10^{20} D^+/cm^2 and 1×10^{21} D^+/cm^2 were used to investigate the process of blister formation at target temperatures of room temperature (RT), 600 and 800 °C, respectively. The erosion yields were determined from the total weight loss of the target measured in situ by a vacuum microbalance with a sensitivity of ± 1 μg. The bombardments with 3 keV D_3^+ were also performed at RT subsequent to the implantation of 4 keV He^+ and 300 eV D_3^+, respectively. The fluences of the prior implanting were $(1–3) \times 10^{17}$ He^+/cm^2 and 6.3×10^{20} D^+/cm^2. For comparison, two polished Mo samples were bombarded with 3 keV D_3^+ up to the same fluence of 1×10^{21} D^+/cm^2 at RT and 800 °C, respectively.

The sputtering yields were determined by the total weight loss of the target. After ion beam bombardment, SEM was used to observe the surface structure, especially the blister formation. The observation was done at an angle of 55° towards the electron detector to increase the contrast of surface structures.

The depth profile of retained deuterium in tungsten was determined by elastic recoil detection (ERD) with 2.6 MeV He^+ on a tandem accelerator. Helium ions were injected at an angle of 75° to the surface normal. The recoiling deuterium was detected in a Si surface barrier mounted at a forward angle of 30° in the laboratory coordinate frame. All the scattered helium particles were stopped by a 5.1 μm thick Ni foil mounted in front of the detector. A thin a-C:D film (30 nm) on Si with naturally absorbed hydrogen was used for energy calibration. The calculations of depth profiles of deuterium in tungsten are based on the procedures described in [9,10].

3. Results

3.1. Fluence dependence

Three samples were bombarded with 1 keV D^+ at RT up to the fluences of 1×10^{19}, 1×10^{20} and 1×10^{21} D^+/cm^2, respectively. SEM images show the ion-induced surface changes in Fig. 1. Compared with the unbombarded surface, the effect of ion fluence on the blister formation at the surface can be clearly seen in

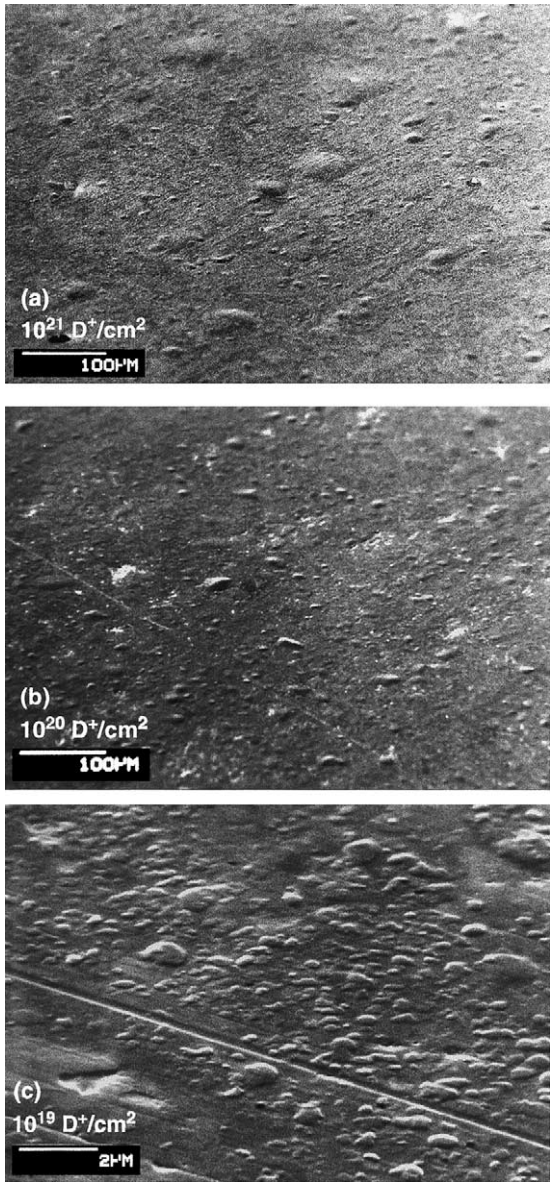

Fig. 1. SEM images of samples bombarded by 1 keV D^+ at RT with different fluences: (a) 1×10^{21} D^+/cm^2; (b) 1×10^{20} D^+/cm^2; (c) 1×10^{19} D^+/cm^2. The scale bar is 100 μm for (a) and (b) and 2 μm for (c).

Fig. 1(a)–(c). The magnification of Fig. 1(c) is a factor of 50 higher than that of Fig. 1(a) and (b). With the increase of ion fluence, the blister size increases and the blister number decreases. Fig. 2 shows the blister size distributions as obtained from Fig. 1 for bombardment with 1×10^{19}, 1×10^{20} and 1×10^{21} D^+/cm^2, respectively. Considering the much smaller counting area for the exposure of 1×10^{19} D^+/cm^2, we took two SEM images from different points in the exposed area of one sample, and counted the blisters to check the homogeneity of the blister formation. The two curves (solid and open squares) shown in Fig. 2 correspond to the two countings of different areas. They agree well in the range of blister diameters larger than 0.2 μm. The high uncertainty for counting small blisters of ≈0.06 μm is mainly induced by the resolution of the SEM system and the inhomogeneity of the small blister distribution at the surface. Fig. 2 shows that the number of blisters induced by 1×10^{19} D^+/cm^2 bombardment is four orders of magnitude higher than that induced by the exposure of 1×10^{20} and 1×10^{21} D^+/cm^2. They are mainly concentrated on the size of ≈0.2 μm and scattered from 0.06 to 1.5 μm. The blister size is much larger for a high fluence bombardment. The blisters, as large as 55 and 75 μm, are found for the exposure of 1×10^{20} and 1×10^{21} D^+/cm^2, respectively.

The three bombarded samples are measured by ERD to get the information about deuterium retention and depth profile in the near surface layer of W. Fig. 3 shows the results. The projected range of 1 keV D^+ in tungsten is about 10 nm and the surface erosion by sputtering as measured from the weight loss of the samples is calculated to be 4.5 nm for 10^{19} D/cm^2 (see Table 1). However, the implanted D diffuses into the depth far beyond from the ion range. The diffusion of D

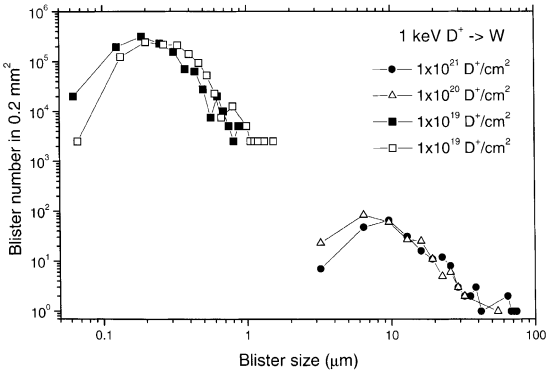

Fig. 2. Blister size (diameter) distribution for the bombardment of 1 keV D^+ at RT with different fluences. Symbols: (●): 1×10^{21} D^+/cm^2; (△): 1×10^{20} D^+/cm^2; and (□, ■): 1×10^{19} D^+/cm^2 (solid and open squares represent two independent measurements at different positions of the same sample).

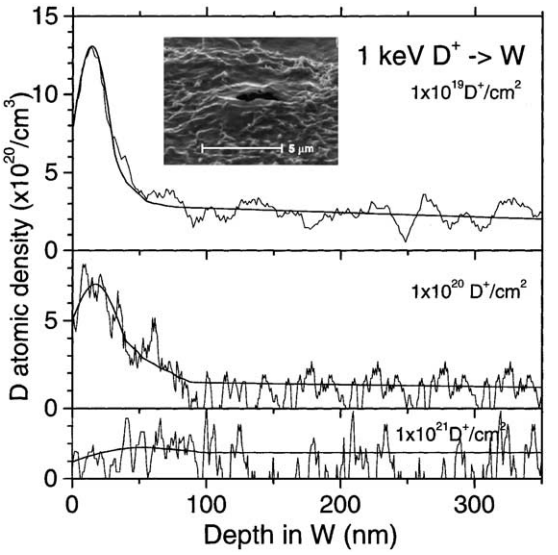

Fig. 3. Depth profile of D in the near surface of W for the bombardment of 1 keV D^+ at RT with different fluences. (—): 1×10^{19} D^+/cm^2; (--): 1×10^{20} D^+/cm^2 and (···): 1×10^{21} D^+/cm^2. The inserted SEM image shows the blister 'Deckeldicke' after a fluence of 1×10^{21} D^+/cm^2.

into W becomes more pronounced with the implanted D fluence. On the other hand, the D atom density retained within the depth of 50 nm decreases with implanted fluences above 10^{19} D/cm^2 as seen in Fig. 3. The inserted SEM image is taken from a tungsten sample after 1 keV D^+ implantation at RT with the fluence of 1×10^{21} D^+/cm^2. From the rupture on the top of the blister, one can deduce a thickness of the cover of the blister – or 'Deckeldicke' – of ≈0.5 μm, about a factor of 100 larger than the ion projected range. The integral retention of D in the near surface layer of 350 nm is 1.5×10^{16}, 8×10^{15} and 7×10^{15} D^+/cm^2 for the bombardment of 1×10^{19}, 1×10^{20} and 1×10^{21} D^+/cm^2, respectively. The mechanism of the decrease of D retention with the increase of implantation fluence will be discussed later.

The appearance and development of blisters on the surface does not seem to have a drastic influence on the erosion yields by sputtering. Sputtering yields obtained from weight loss measurements are given in Table 1 for different energies and fluences. Although the lowest fluences yield weight losses not much above the reproducibility of the micro-balance, there is no concernible fluence dependence of the erosion yield for 200 eV and 1 keV bombardment.

3.2. Energy dependence

Fig. 4 shows the SEM image taken from W samples after D bombardment at RT up to the fluence of

Table 1
Erosion yields of W for D ion bombardment as obtained from weight loss measurements

Energy (eV)	Fluence (D^+/cm^2)	Yield at		
		20 °C	600 °C	800 °C
1000	1×10^{21}	2.87×10^{-3}	4.1×10^{-3}	3.65×10^{-3}
		2.85×10^{-3}		
	1×10^{20}	2.47×10^{-3}		
	After He prebomb.	2.5×10^{-3}		
	1×10^{19}	$(1.1 \pm 1) \times 10^{-3}$		
200	1×10^{21}	1.9×10^{-4}		
	1×10^{20}	$<1 \times 10^{-4}$		
100	1×10^{21}	$<7 \times 10^{-5}$		8.4×10^{-4}
		$<5.3 \times 10^{-5}$		

1×10^{21} D^+/cm^2 with different energies of 100 eV, 200 eV and 1 keV, respectively. The magnification of Fig. 4(a) and (b) is a factor of 5 higher than Fig. 4(c). Clearly, the blister size increases with the bombardment energy. The blister size distribution is shown in Fig. 5. The blisters are counted in an area as large as that for Fig. 2. The small blisters formed due to the exposure at low energy of 100 eV are counted for two different areas (solid and open squares in the figure) to demonstrate the degree of reproducibility as described for Fig. 2. The blister number for the exposure at 100 eV is 2 and 3 orders of magnitude higher than that for the exposure at 200 eV and 1 keV, respectively. The blisters are mainly concentrated on the size of 0.4 μm with a variation of 0.13–1.9 μm for 100 eV exposure. The blister size increases to 0.6–9 μm and 3–75 μm for the bombardment at 200 eV and 1 keV, respectively.

Two unpolished W samples are bombarded by D^+ at RT with energies of 100 eV and 1 keV, respectively, up to the same fluence of 1×10^{21} D^+/cm^2. No blisters are found for 100 eV D^+ bombardment. For the sample bombarded with 1 keV D^+, we only find five large blisters with the size of 200, 150, 100, 70 and 8 μm after careful observation in the whole bombarded area. No small blisters are formed due to the surface roughness.

3.3. Temperature dependence

Two tungsten samples are bombarded with 1 keV D^+ up to the fluence of 1×10^{21} D^+/cm^2 at different temperatures of RT and 800 °C, respectively. Fig. 6 shows the SEM images. From the low magnification in Fig. 6(a) in comparison with Fig. 4(c), we can see clearly that there are no large blisters formed at the W surface due to the bombardment at 800 °C. The sputtering yields, determined from the total in situ weight loss, are 2.86×10^{-3} atoms/ion (average value from three samples) at RT, and increases to 3.65×10^{-3} atoms/ion at 800 °C (Table 1). The surface erosion can been observed clearly from the high magnifications of Fig. 6(b) and (c). The small blisters that are formed during the bombardment at low fluence at RT shown in Fig. 1(c) are sputtered away during further bombardment. We can see many sharp erosion cones in Fig. 6(c). The largest cones are ≈0.6 μm high. This suggests that a W surface layer of $\geqslant$0.6 μm has been eroded. This is similar to the value of ≈0.66 μm calculated from the sputtering yield. No cones have been observed in Fig. 6(b) at enhanced temperature of 800 °C. The surface structure shown in Fig. 6(b) is similar to the surface of Mo after D^+ bombardment with a high fluence of 1×10^{21} D^+/cm^2 [11]. It shows clearly the grain structure of W due to the different erosion yields on different grain orientations. The bombardment of W with 1 keV D^+ at 600 °C is also performed up to the fluence of 1×10^{20} D^+/cm^2. No blisters are observed.

Although no change in surface structure is observed in the SEM the erosion yields given in Table 1 indicate a slight increase with the target temperature. Especially at the lowest energy of 100 eV D^+, an energy below the threshold of physical sputtering, where no erosion could be observed at RT within the sensitivity of the measurements, an increase to a small, but clearly measurable weight loss occurs at 800 °C. This may be due to the desorption of surface oxides formed in the residual gas of our experiment ($\leqslant 10^{-7}$ mbar oxygen partial pressure). This influence of oxygen is only measurable at ion energies close or below the threshold energy for sputtering [12,13].

3.4. Double bombardment

In order to simulate conditions where different ion species at different energies bombard the surface, two double bombardment experiments were performed at RT: (1) 4 keV He^+ with the fluence of $1–3 \times 10^{17}/cm^2$ prior to the bombardment of 1 keV D^+ up to the fluence of $1 \times 10^{20}/cm^2$ (Fig. 7(a) and (b)); (2) 100 eV D^+ with the fluence of $6.3 \times 10^{20}/cm^2$ prior to the bombardment of 1 keV D^+ up to the fluence of 1×10^{21} D^+/cm^2 (Fig. 4(a), Fig. 1(a), Fig. 7(c)). The SEM images in Fig. 7 show the He pre-implantation

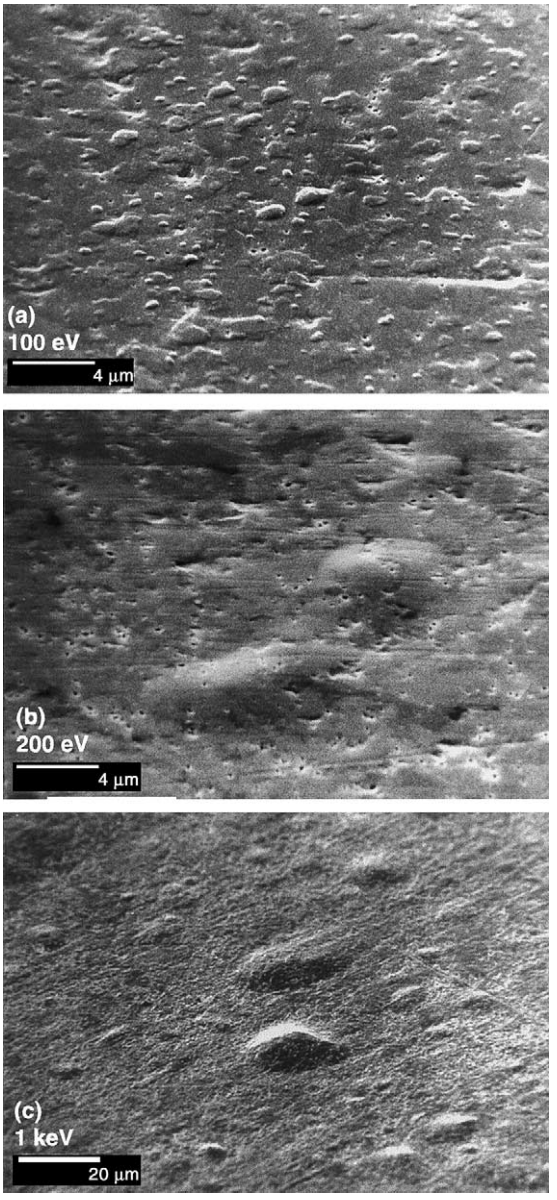

Fig. 4. SEM images of samples bombarded by D^+ at room temperature with a fluence of 1×10^{21} D^+/cm^2 at the energy of (a) 100 eV; (b) 200 eV and (c) 1 keV. The scale bar is 4 μm for (a) and (b) and 20 μm for (c).

(a) and the double implantations (b) and (c), respectively. Fig. 8 shows the depth profiles of the deuterium atom density in the near surface layer of W due to double bombardment (dashed lines in Fig. 8(a) for $He^+ + D^+$ and in Fig. 8(b) for $D^+ + D^+$). The profiles of D due to single 1 keV D^+ bombardment with a fluence of $1 \times 10^{20}/cm^2$ (solid line in Fig. 8(a)) and $1 \times 10^{21}/cm^2$ (solid line in Fig. 8(b)) are added for comparison.

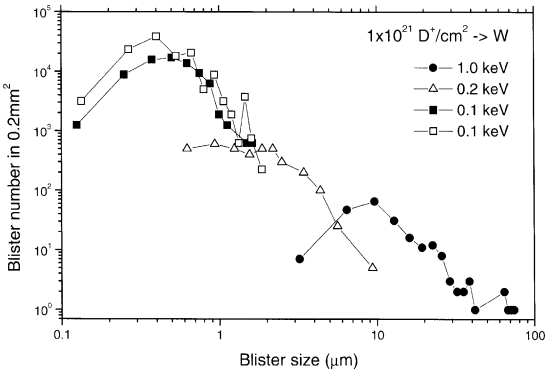

Fig. 5. Blister size (diameter) distribution for the bombardment of D^+ at RT with a fluence of 1×10^{21} D^+/cm^2 at different energies. Symbols: (●): 1 keV; (△): 200 eV; and (□, ■): 100 eV (solid and open squares represent two independent measurements at different positions of the same sample).

For the first double bombardment experiment ($He^+ + D^+$), we found small blisters, 0.1–0.45 μm in diameter, induced by the pre-bombardment of 4 keV He^+ with the fluence of $3 \times 10^{17}/cm^2$ in Fig. 7(a) as reported earlier for Nb [1]. The large blisters induced by the 1 keV D^+ bombardment with a fluence of $1 \times 10^{20}/cm^2$ shown in Fig. 1(b) have been described in Section 3.1. However, no such blisters were observed for the double bombardment shown in Fig. 7(b). An observation at higher magnification (not given here) shows that small blisters are not formed either, and the surface modification is similar to that induced only by D^+ bombardment. The depth profile of D shows remarkable changes due to the double bombardment. At the depth of ≈25 nm from the surface the D atom density increases by a factor of 8 (Fig. 8(a)). The D retention within the depth range of 350 nm in the near surface layer of W increases up to the value of 5.62×10^{16} D^+/cm^2 for the double bombardment of 1 keV D^+ with $1 \times 10^{20}/cm^2$ after the bombardment of 4 keV He^+ with $1 \times 10^{17}/cm^2$. Compared with the single bombardment of 1 keV D^+ with $1 \times 10^{20}/cm^2$, the integral D retention is enhanced by a factor of 7.2.

For the second double bombardment experiment ($D^+ + D^+$), the small blister induced by 100 eV D^+ bombardment (Fig. 4(a)) and the large blisters induced by 1 keV D^+ bombardment (Fig. 1(a)) have been described in Sections 3.1 and 3.2. No blisters are found after the double bombardment shown in Fig. 7(c). Similarly, no small blisters are found in a high magnification SEM image (not submitted here) either, and the surface erosion is similar to that induced by only 1 keV D^+ bombardment with a high fluence of $1 \times 10^{21}/cm^2$. At the depth of 25 nm from the surface the D atomic density increases a factor of 7 (Fig. 8(b)) due to the double bombardment. The D retention within the depth

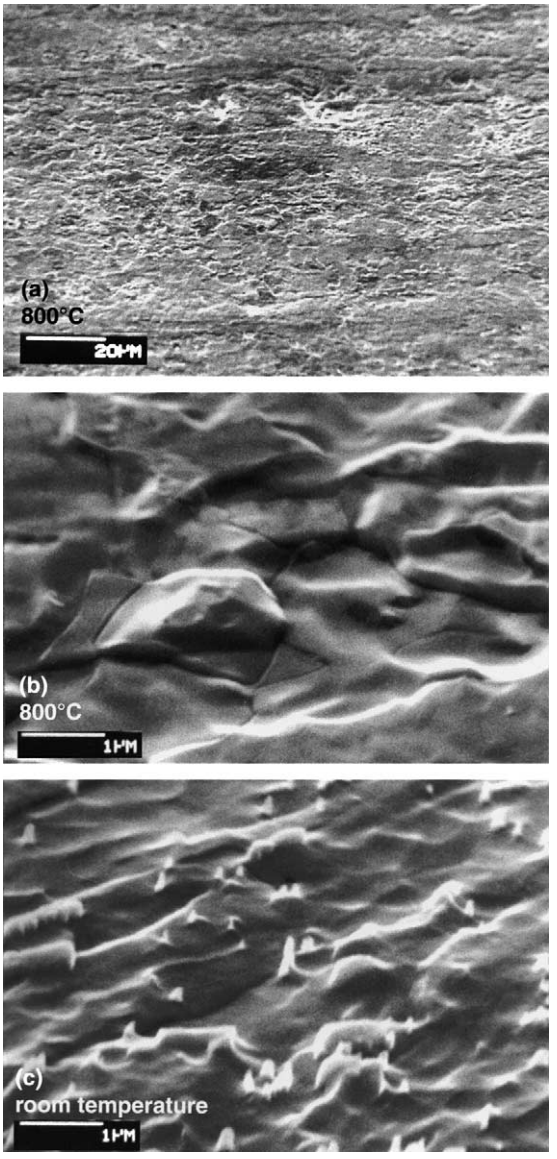

Fig. 6. SEM images of tungsten samples bombarded by 1 keV D^+ up to the fluence of 1×10^{21} D^+/cm^2 at different temperatures and with different magnifications. (a) and (b): at 800 °C with scale bars of 20 and 1 μm, respectively, and (c) at RT with a scale bar of 1 μm.

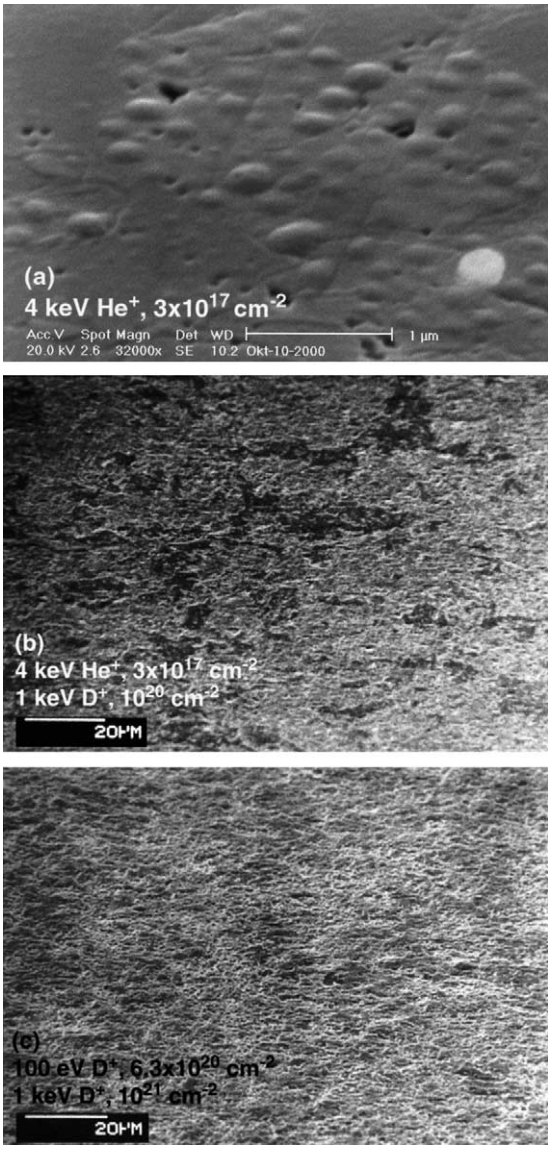

Fig. 7. SEM images of W samples subjected to two different double bombardments at RT. The first group: (a) single bombardment of 4 keV He^+ with the fluence of $3 \times 10^{17}/cm^2$; (b) double bombardment of (a) prior to 1 keV D^+ at 10^{20} D/cm^2 (compare to Fig. 1b). The second group: (c) double bombardment of 100 eV D^+ with the fluence of $6.3 \times 10^{20}/cm^2$ (see Fig. 4(a)) prior to 1 keV D^+ at $10^{21}D/cm^2$ (compare to Fig. 1(a)).

of 350 nm in the near surface layer increases to 3.01×10^{16} D^+/cm^2. This is an increase of a factor of 4.2 compared to a bombardment with 1 keV D^+ with $1 \times 10^{20}/cm^2$ only.

3.5. Comparison with Mo

No blistering was observed on the surface of Mo after 1 keV D^+ bombardment with the fluence of 1×10^{21} D^+/cm^2 at both RT and 800 °C. The surface structure exhibits large differences in the erosion yield for different grain orientations as reported already in [11]. The average sputtering yields are 8.38×10^{-3} for RT and 1.10×10^{-2} for 800 °C. These are abound a factor of three higher than the values for W (2.86×10^{-3} for RT and 3.65×10^{-3} for 800 °C).

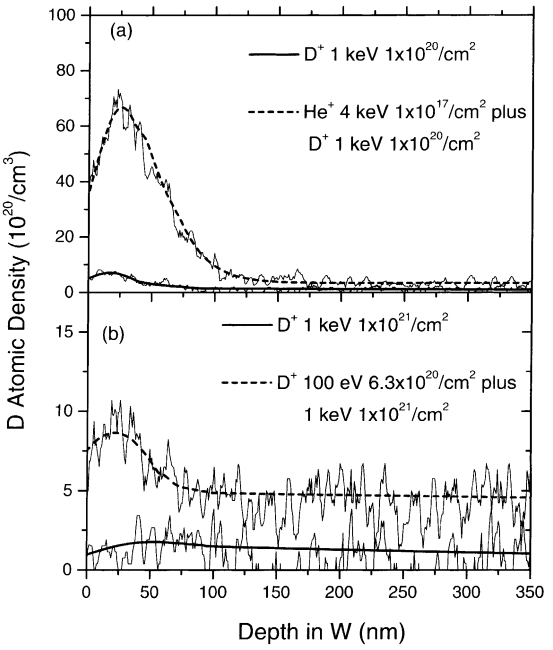

Fig. 8. Depth distribution of the D atomic density in the near surface layer of W due to double bombardment at RT. (a) (--): 4 keV He^+ with the fluence of $1 \times 10^{17}/cm^2$ prior to the bombardment of 1 keV D^+ up to the fluence of $1 \times 10^{20}/cm^2$; (—): single bombardment of 1 keV D^+ up to the fluence of $1 \times 10^{20}/cm^2$ for comparison. (b) (--): 100 eV D^+ with the fluence of $6.3 \times 10^{20}/cm^2$ prior to the bombardment of 1 keV D^+ up to the fluence of $1 \times 10^{21}/cm^2$; (—): single bombardment of 1 keV D^+ up to the fluence of $1 \times 10^{21}/cm^2$.

4. Discussion

The mechanism for blister formation was under active discussion for the case of He implantation into metals [2]. He forms gas bubbles in metals, such as Nb, where the gas pressure is not in equilibrium but much higher than the surface tension. Upon further implantation the bubbles grow by mechanisms such as loop punching [14] until they interconnect and separate from the bulk at a depth equivalent to the projected ion range. Deviations of the blister lid thickness – Deckeldicke – as well as the observation of large compressive stresses in the implanted layer, which are released upon blistering, lead alternatively to the model of stress driven blistering. The relation of the diameter of the blisters to the Deckeldicke could perfectly be explained by a theory describing the buckling of plates under compressive stresses [15,16]. It can be concluded that in the case of He the Deckeldicke is given roughly by the ion range while the final blister size is determined by the accumulated compressive stresses in the layer.

For the case of D in W the observed Deckeldicke is much larger, by about a factor of 100, than the projected ion range. D is known to diffuse far beyond the range [17] and get trapped at defects and dislocations induced by the ion irradiation. A layer much thicker than the ion range contains defects and trapped D and must be assumed to experience large stresses. In this case there is no evidence from the depth profiles for gas accumulation in cavities at the large depths where the blisters are formed. Therefore, stress must be assumed as driving force for blistering. The large blister diameter is also in agreement with large Deckeldicke within the plate theory [15,16,18]. The increase of the blister size with the implantation fluence reflects the increase in the stressed layer thickness with inward diffusion of the deuterium.

In addition at 1 keV, tungsten is increasingly sputtered with increasing fluence. It is concluded from the weight loss of the samples that a surface layer larger than the ion range is sputtered at a fluence of 1×10^{21} D^+/cm^2, thus erasing the high D concentration close to the surface as seen from Fig. 3. Further implantation does not lead to a similar accumulation of D. It must be concluded that sputter erosion, combined with the disappearance of the smaller blisters, changes the material structure such as to provide microchannels for the release of near-surface implanted deuterium. Within the analyzed surface layer, which is restricted to about 350 nm for ion beam analysis, the retained amount of deuterium effectively decreases although results from thermal desorption spectroscopy [3] shows a gradual increase of the total retained amount.

Double implantation changes the trapping conditions for the subsequently injected deuterium. The surface layer containing He bubbles and blisters provides ample surface near trapping sites for deuterium as can be seen from Fig. 8(a). Low energy D pre-implantation behaves similarly, thus preventing the formation of large blisters typical for 1 keV D^+. This surface-near layer will be sputtered away at high fluences: 10^{21} D^+/cm^2 at 1 keV is equivalent to the erosion of 1 μm of material. The absence of blisters at the higher fluence shows that no second generation of blisters is formed after sputtering of a blistered surface layer. The measured sputtering yields at fluences above 10^{19} D^+/cm^2 do not depend on fluence.

5. Conclusions

In the present study, an experimental investigation on the blister formation of W and Mo is performed as a function of ion energy, ion fluence and target temperature, and the following conclusions can be made.

1. Systematic fluence dependent experiments show that blister formation on W at RT occurs at fluences as low as 10^{19} cm^{-2} for 1 keV D^+. The size of the blisters increases with increasing fluence.

2. Systematic ion energy dependent experiments show that the blister formation is observed at ion energies as low as 100 eV at RT and a fluence of 10^{21} cm^{-2}. The size of the blisters increases with increasing ion energy.
3. It is found, that there is no blister formation on W at a target temperature $\geqslant 600$ °C (1 keV D^+, fluence of 10^{21} cm^{-2} s^{-1}).
4. A preliminary result shows, that the damage of He ions may increase the D-retention via implantation at the W surface.
5. No blister formation has been observed on Mo at RT and 800 °C, D^+ energy of 1 keV and a fluence of 10^{21} cm^{-2} s^{-1}.
6. It is interesting to note that there are several conditions where blistering on W can be avoided. This study showed, that there is no blister formation at target temperatures of W $\geqslant 600$ °C and after after dual-energy irradiation. Also, on unpolished technical surfaces blisters do not form or are too small to be visible in the SEM.

However, these experiments have been performed at relatively low flux densities $\leqslant 10^{16}$ cm^{-2} s^{-1}, which are certainly relevant for first wall conditions but not for divertor conditions $\geqslant (10^{19}$ cm^{-2} $s^{-1})$. Therefore, further detailed experimental investigations at high flux density are urgently required for more accurate assessments.

References

[1] J. Roth, in: Inst. Phys. Conf. Ser., vol. 28, 1976, p. 280 (Chapter 7).
[2] B.M.U. Scherzer, in: R. Behrisch (Ed.), Sputtering by Particle Bombardment II, Springer, Berlin, 1983.
[3] A.A. Haasz, M. Poon, J.W. Davis, J. Nucl. Mater. 266–269 (1999) 520.
[4] T. Venhaus, T. Abeln, R. Doerner, R. Causey, J. Nucl. Mater. 290–293 (2001) 505.
[5] F.C. Sze, L. Chousal, R.P. Doerner, S. Luckhardt, J. Nucl. Mater. 266–269 (1999) 1212.
[6] V.Kh. Alimov, K. Ertl, J. Roth, K. Schmid, in: 5th International Workshop on Hydrogen Isotopes in Solids, May 17–19, 2000, Stockholm, Sweden, Phys. Scripta T94 (2001) 34.
[7] R. Causey, K. Wilson, T. Venhaus, W.R. Wampler, J. Nucl. Mater. 266–269 (1999) 467.
[8] W. Eckstein, C. García-Rosales, J. Roth, W. Ottenberger, IPP report 9/82, February, 1993.
[9] A. Turos, O. Meyer, Nucl. Instr. and Meth. B 4 (1984) 92.
[10] F. Besenbacher, I. Stensgaard, P. Vase, Nucl. Instrum. and Meth. B 15 (1986) 459.
[11] H.L. Bay, J. Roth, J. Bohdansky, J. Appl. Phys. 48 (1977) 4722.
[12] J. Roth, J. Bohdansky, W. Ottenberger, Max-Planck-Institut für Plasmaphysik, Report IPP 9/26, 1979.
[13] E. Hechtl, W. Eckstein, J. Roth, J. Laszlo, J. Nucl. Mater. 179–181 (1991) 290.
[14] J.H. Evans, J. Nucl. Mater. 76&77 (1978) 228.
[15] M.R. Risch, J. Roth, B.M.U. Scherzer, in: Proceedings of the International Symposium on Plasma Wall Interaction, Jülich, 1976, Pergamon, London, 1977, p. 353.
[16] E.P. EerNisse, S.T. Picraux, J. Appl. Phys. 48 (1977) 9; Erratum 48 (1977) 2468.
[17] V.Kh. Alimov, K. Ertl, J. Roth, J. Nucl. Mater. 290–293 (2001) 389.
[18] W. Timoshenko, S. Woinowsky-Krieger, Theory of Plates and Shells, McGraw-Hill, New York, 1959.